

Carbon Dioxide (CO₂) Sequestration of Mangrove Forests Using Remote Sensing in Trusan Kinabatangan Sabah, Malaysia

Mohd Arif Shahdan Azmi ¹, Maizaitoldura Mohd Isa, Mckreddy Yaban and Muhammad Fikri

Razali

Malaysian Space Agency (MYSA): Research Officer

arifshahdan@mysa.gov.my

ABSTRACT: *Mangrove ecosystems are valuable for reducing climate change because they can absorb and store carbon dioxide (CO₂). Their ability to absorb CO₂ at a rate three times higher than terrestrial forests and tropical rainforests highlights their importance in our efforts to combat rising greenhouse gas emissions. Mangrove forests along Trusan Kinabatangan Sabah, Malaysia, are incredibly valuable ecosystems with high potential for carbon storage, coastal buffer zones, tourism, and the fishing industry. This study focuses on the carbon dioxide sequestration capabilities of the mangrove forests in Trusan Kinabatangan, Sabah, Malaysia, utilizing remote sensing technologies. Forest cover mapping is effectively facilitated through the implementation of remote sensing techniques using high-resolution images, advanced image processing, and geographic information systems (GIS). In addition, the study introduces a method for calculating CO₂ absorption in forest ecosystems using Landsat satellite imagery. The approach involves the classification of land cover to identify forested areas and the application of vegetation indices, such as the Normalized Difference Vegetation Index (NDVI), to estimate aboveground biomass. Biomass estimates are converted to carbon stock using established allometric equations, and changes in carbon stock over time are analyzed to determine the rate of CO₂ sequestration. A comparison has been made of the estimated CO₂ absorption rates for the years 2018, 2020, and 2023. The study findings for 2018 indicate that CO₂ sequestration rate of Trusan Kinabatangan, Sabah, derived from remote sensing data, is approximately 98.32 tons of carbon per hectare in 2018, 112.30 tons of carbon per hectare in 2020 and 124.73 tons of carbon per hectare in 2023. Comparatively, from 2018 to 2023, biomass accumulation significantly increases by 26.41 tons of carbon per hectare or 27% in a similar area. These results highlight significant variations or similarities in biomass accumulation and carbon sequestration rates.*

Keywords: *Mangrove, Carbon Dioxide (CO₂), Geographical Information Systems (GIS), Normalized Difference Vegetation Index (NDVI)*

Introduction

Among the planet's most productive and biologically varied ecosystems are mangrove forests. They are essential to the global carbon cycle because of their extraordinary capacity to retain and store carbon dioxide (CO₂) both above and below ground. According to certain studies, these special coastal ecosystems may sequester carbon at rates up to four times larger than terrestrial forests, demonstrating their exceptional efficiency in doing so (Donato et al., 2011). Because of this, mangroves play vital role and significant for reducing the effects of climate change, especially in tropical and subtropical area. Mangrove forests offer variety of ecosystem services, such as carbon sequestration, coastal protection, and as habitat for a wide range of wildlife which may be found at Trusan Kinabatangan, Sabah, Malaysia. Despite their significance, these forests are in danger due to land conversion, deforestation, human activity, and climate change. As a result, it is critical to monitor and manage them using precise and effective approaches.

The most accurate approach to gather biomass data, according to Lu (2006), is by field data collection, yet this approach is costly, labour-intensive, time-consuming, and challenging to carry out in large, isolated areas. As a result, another way to collect this data involves using remote sensing technologies and an aerial approach. In addition, to mapping the geographical extent and density of mangrove forests which are crucial for determining total biomass remote sensing provides strong tools for estimating CO₂ sequestration in mangrove areas and providing vital information for conservation and climate mitigation initiatives Researchers can use satellite imaging and other remote sensing data to evaluate the spatial extent, structure, health, and carbon storing capacity of forests with great precision (Fatoyinbo et al., 2008).

High-resolution data that remote sensing provides can be used to assess the size, composition, and condition of mangrove ecosystems. Inaccessible landscapes may now be analyzed thanks to remote sensing technology, which provides vital information for improving and informing conservation and management plans. Furthermore, the amalgamation of various remote sensing technologies allows researchers to attain exceptionally comprehensive and precise evaluations of mangrove carbon stores, and precisely tracking their temporal fluctuations. Mangrove ecosystems are crucial in halting climate change because they may store up to four times as much carbon per hectare as tropical forests. Satellite images and LiDAR are two handy remote sensing tools for calculating above-ground biomass and calculating the carbon stores below the surface in these regions. With the use of these technologies, deforestation, degradation, and other changes may be continuously monitored, enabling prompt responses to protect these ecosystems rich in carbon. Satellite imaging time-series analysis is helpful in tracking changes in mangrove cover and identifying regions undergoing restoration or deterioration. With remote sensing methods, this study seeks to determine the mangrove forests

capacity for sequestering CO₂ in Trusan Kinabatangan, Sabah, Malaysia.

Literature Review

Mangrove forests, referred to as "blue carbon" are among the planet's most productive ecosystems because of their great ability to sequester carbon. Mangrove forests can absorb carbon dioxide (CO₂) from the atmosphere and store it in their biomass and sediment which significantly contributes to the mitigation of climate change. Moreover, their wet and anoxic soils slow down decomposition processes and improve long-term carbon storage; mangroves are thought to store up to four times more carbon per unit area than terrestrial forests (Alongi, 2014).

Mangrove forests are known for their capacity to sequester carbon because of their adaptation to saline environments and geographical location. Nevertheless, it is difficult to precisely estimate their capacity to store carbon at both local and global scales locally and globally. One potential method for mapping, monitoring, and calculating carbon sequestration in these ecosystems is by using remote sensing technologies. Through the storage of organic carbon in both above-ground biomass (tree trunks, branches, and leaves) and below-ground biomass (roots and soil), mangroves considerably contribute to CO₂ sequestration. Mangroves can store between 900 and 1,500 tons of carbon per hectare, according to studies (Donato et al., 2011). Their capacity to store carbon in submerged soils, where organic matter is preserved for generations, accounts for their great sequestration potential.

Furthermore, preserving and monitoring these ecosystems is crucial since the deterioration and deforestation of mangrove forests may cause the released carbon to return to the atmosphere. Remote sensing technologies are now essential for monitoring changes in mangrove cover and determining the dynamics of their carbon supply. The evaluation of mangrove ecosystems has significantly benefited from the use of remote sensing methods such as satellite images, aerial photography, LiDAR (Light Detection and Ranging), and UAV (Unmanned Aerial Vehicle). These instruments enable extensive, long-term mangrove forest monitoring and offer crucial information about these ecosystems' biomass and carbon storage potential. Mapping and monitoring mangrove forests can be done effectively and economically with the use of satellite-based remote sensing. Mangrove forest cover mapping and biomass calculation have been accomplished through various studies by using multiple satellite missions, such as Sentinel, MODIS, and Landsat. Vegetation indices like the Enhanced Vegetation Index (EVI) and Normalized Difference Vegetation Index (NDVI) are frequently used to interpret mangrove biomass and carbon stocks (Giri, 2016).

While remote sensing offers many benefits, there are several obstacles to precisely quantifying mangrove carbon stores. Differentiating between mangrove species is a major challenge since they may have differing capacities for sequestering carbon. In addition, a significant amount of the total carbon stored in mangroves is represented by below-ground biomass, which is frequently difficult for satellite data to capture. Field-based measurements are required to estimate below-ground carbon stocks and to validate and supplement data obtained from remote sensing (Atwood et al., 2017). Ground-truthing initiatives guarantee that carbon stock estimates accurately reflect the potential for mangrove ecosystems to sequester carbon and assist in enhancing the accuracy of remote sensing models. Besides, the creation of long-term monitoring programs employing cutting-edge satellite platforms will offer vital information about how human activity and climate change affect mangrove carbon reserves over time.

Methodology

2.1 Study Region

Mangrove forests are vital to coastal ecosystems, offering habitat to numerous species and shielding coastlines from erosion. This study, covering 510 hectares in the Trusan Kinabatangan Forest Reserve area of Sabah, Malaysia, underscores the significance of these forests for biodiversity and ecological balance in the region. The study extends from $5^{\circ} 51' 1.8396''$ to $5^{\circ} 35' 0.0852''$ latitude and $118^{\circ} 13' 47.6688''$ to $118^{\circ} 37' 52.3164''$ longitude. This area is predominantly covered by mangrove trees, which play a crucial role in coastal protection and carbon sequestration. However, it also experiences various development activities, including the expansion of villages, which often leads to habitat loss. Additionally, tourism ventures can put pressure on these ecosystems through increased foot traffic and infrastructure development. Aquaculture operations, such as shrimp farming, further impact mangrove areas by altering water quality and land use. These factors combined can significantly affect the health and sustainability of mangrove ecosystems.

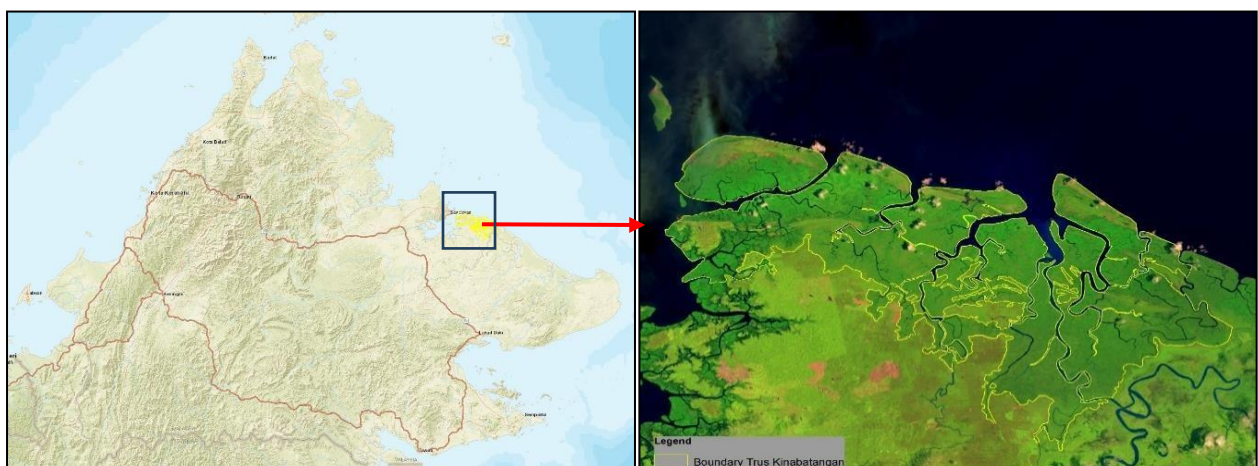


Figure 1: Study Area

2.2 Image Acquisition

The acquired data was from Landsat 8, which was launched from Vandenberg Air Force Base, California on February 11, 2013 (U.S. Department of the Interior, 2022). The satellite consists of Operational Land Imager (OLI) and Thermal Infrared Sensor (TIRS). Level 2 imageries were downloaded from the <https://earthexplorer.usgs.gov/> website.

Table 1: Landsat 8 bands

Band Name	Wavelength Range (μm)	Resolution (m)
Band 1 Coastal Aerosol	0.43 - 0.45	30
Band 2 Blue	0.45 - 0.51	30
Band 3 Green	0.53 - 0.59	30
Band 4 Red	0.64 - 0.67	30
Band 5 Near-Infrared	0.85 - 0.88	30
Band 6 SWIR 1	1.57 – 1.65	30
Band 7 SWIR 2	2.11 – 2.29	30
Band 8 Panchromatic	0.50 - 0.68	15
Band 9 Cirrus	1.36 – 1.38	30
Band 10 TIRS	10.6 – 11.19	100
Band 10 TIRS	11.5 – 12.51	100

2.3 REMOTE SENSING DATA

Multiple date Landsat 8 OLI imageries were used. The Landsat 8 satellite is the latest generation of terrestrial remote sensing satellites. Its sensors have been significantly improved in terms of imaging mode, band settings and signal-to-noise ratio. Satellite data from 2018 to 2023 with different seasons were collected and processed. Landsat 8 has better sensors with more bands for detailed images. It offers improved accuracy and fewer data gaps. The new bands include coastal and cirrus cloud measurements. It also has better calibration for higher quality data. High-resolution imagery and advanced sensors provide valuable insights into environmental changes and human activities, supporting both scientific research and practical applications in natural resource management.

Table 2: Summary of the satellite remote sensing data used in this study

Type of Data	Image Date
Landsat 8 Operational Land Imager(OLI)	16 June 2023
	6 November 2020
	29 August 2018

2.4 RADIOMETRIC CORRECTION

Radiometric correction in Landsat 8 is essential for improving the accuracy of satellite imagery. The process adjusts for various factors that can distort the recorded data, ensuring that the brightness values in the images reflect the actual conditions on Earth's surface. The correction process begins with calibration, where raw digital numbers (DNs) from the sensor are converted into physical units like radiance or reflectance. This is done using calibration coefficients specific to Landsat 8's sensors. Next is atmospheric correction, which removes the effects of atmospheric gases and particles that can distort the measurements, ensuring that the data accurately represents the surface characteristics. Lastly, sensor correction addresses any sensor-specific issues, such as systematic errors or drift, to maintain consistency across images and over time. Correction to Top of Atmosphere changed the pixel values of the image into the reflectance values by normalizing the angle and intensity of solar energy, while the DOS correction intended to remove atmospheric path radiance. DOS correction assumes that there is a pixel containing 0% reflectance.

TOA (Top of Atmospheric) spectral radiance was calculated using the following equation.

$$\text{TOA (L)} = \text{ML} * \text{Qcal} + \text{AL} \quad (1)$$

where:

ML = Band-specific multiplicative rescaling factor from the metadata

Qcal = Quantized and calibrated standard product pixel values (DN)

AL = Band-specific additive rescaling factor from the metadata

Reflective band DN's can be converted to TOA reflectance using the rescaling coefficients in the MTL file:

$$\rho\lambda' = M\rho Qcal + A\rho \quad (2)$$

where:

$\rho\lambda'$ = TOA planetary reflectance, without correction for solar angle. Note that $\rho\lambda'$ does not contain a correction for the sun angle.

$M\rho$ = Band-specific multiplicative rescaling factor from the metadata

(REFLECTANCE_MULT_BAND_x, where x is the band number)

$A\rho$ = Band-specific additive rescaling factor from the metadata

(REFLECTANCE_ADD_BAND_x, where x is the band number)

Q_{cal} = Quantized and calibrated standard product pixel values (DN)

TOA reflectance with a correction for the sun angle is then:

$$P_{\lambda} = \frac{\rho_{\lambda'}}{\cos(\theta_{SZ})} = \frac{\rho_{\lambda'}}{\sin(\theta_{SE})} \quad (3)$$

where:

ρ_{λ} = TOA planetary reflectance

θ_{SE} = Local sun elevation angle. The scene center sun elevation angle in degrees is provided in the metadata

(SUN_ELEVATION).

θ_{SZ} = Local solar zenith angle; $\theta_{SZ} = 90^{\circ} - \theta_{SE}$

2.5 CLASSIFICATION

2.5.1 Land Cover

Landsat imagery from the years 2018, 2020, and 2023 was analyzed and classified into three primary land cover categories namely Mangrove, Urban, and Waterbody using the Support Vector Machine (SVM) classifier.

The Support Vector Machine is a supervised machine learning algorithm used for classification and regression tasks. In this context, SVM was employed to distinguish between different land cover types based on the spectral features extracted from the Landsat images.

2.5.2 Vegetation Index

NDVI image was generated using the following equation.

$$NDVI = (\text{Band 5} - \text{Band 4}) / (\text{Band 5} + \text{Band 4}) \quad (4)$$

The proportion of vegetation (P_v) was then calculated.

$$P_v = \text{Square} ((NDVI - NDVI_{\min}) / (NDVI_{\max} - NDVI_{\min})) \quad (5)$$

Emissivity (ϵ) was calculated using the following equation.

$$\epsilon = 0.004 * P_v + 0.986 \quad (6)$$

where:

the value of 0.986 corresponds to a correction value of the equation.

Vegetation Indices (VI)

The Vegetation Indices were calculated in ArcGIS using the formula as shown below:

$$\text{NDVI} = [\text{NIR}-\text{RED}] / [\text{NIR}+\text{RED}] \quad (7)$$

$$\text{DBI} = [\text{SWIR}-\text{NIR}] / [\text{SWIR}+\text{NIR}] \quad (8)$$

$$\text{MNDWI} = [\text{Green} - \text{SWIR}] / [\text{Green} + \text{SWIR}] \quad (9)$$

2.5.3 Above Ground Biomass (AGB) Estimation

Estimation of above the ground surface biomass value was done using the approach of NDVI result of equation correlation with Above Ground Biomass (AGB) of mangrove that is equal to 0.787 by Jha et al. (2015) as follows:

$$\text{AGB} = 305.9 * \text{NDVI}^{4.864} \quad (10)$$

NDVI = the value of Vegetation Index, AGB = the Above Ground Biomass Value (ton ha⁻¹).

2.5.4 Below Ground Biomass (BGB) Estimation

The estimated value of Below Ground Biomass (BGB) is obtained from the estimation of AGB which is formulated using the equation compiled by Cairns, et al (1997) as follows:

$$\text{BGB} = \exp(-1.0587 + 0.8836 * \text{Ln}(\text{AGB})) \quad (11)$$

AGB = the value of Above Ground Biomass (ton ha⁻¹), BGB = the Below Ground Biomass value (ton ha⁻¹).

2.5.5 Total Accumulated Biomass (TAB)

Total Accumulation Biomass (TAB) is formulated by using:

$$\text{TAB} = \text{AGB} + \text{BGB} \quad (12)$$

TAB = Total Accumulated Biomass (ton ha⁻¹).

2.5.6 Total Carbon Stock (TCS) calculation

Calculation of total carbon stock based on Westlake (1963) using the following formula:

$$TCS = TAB * \% C \text{ organic} \quad (13)$$

TCS = the value of Total Carbon Stock (ton C ha¹), TAB = the value of Total Accumulated Biomass (ton ha¹), %C organic = the percentage value of carbon stock (0.47)

2.5.7 Amount of CO₂ Sequestration (ACS) Calculation

IPCC (2001) suggests converting carbon stock from biomass to carbon dioxide uptake using the following conversion

$$ACS = 3.67 * TCS \quad (14)$$

ACS = the Amount of CO₂ Sequestration (ton C ha¹), TCS = the value of Total Carbon Stock (tonC ha¹).

2.6 RESEARCH FLOW CHART

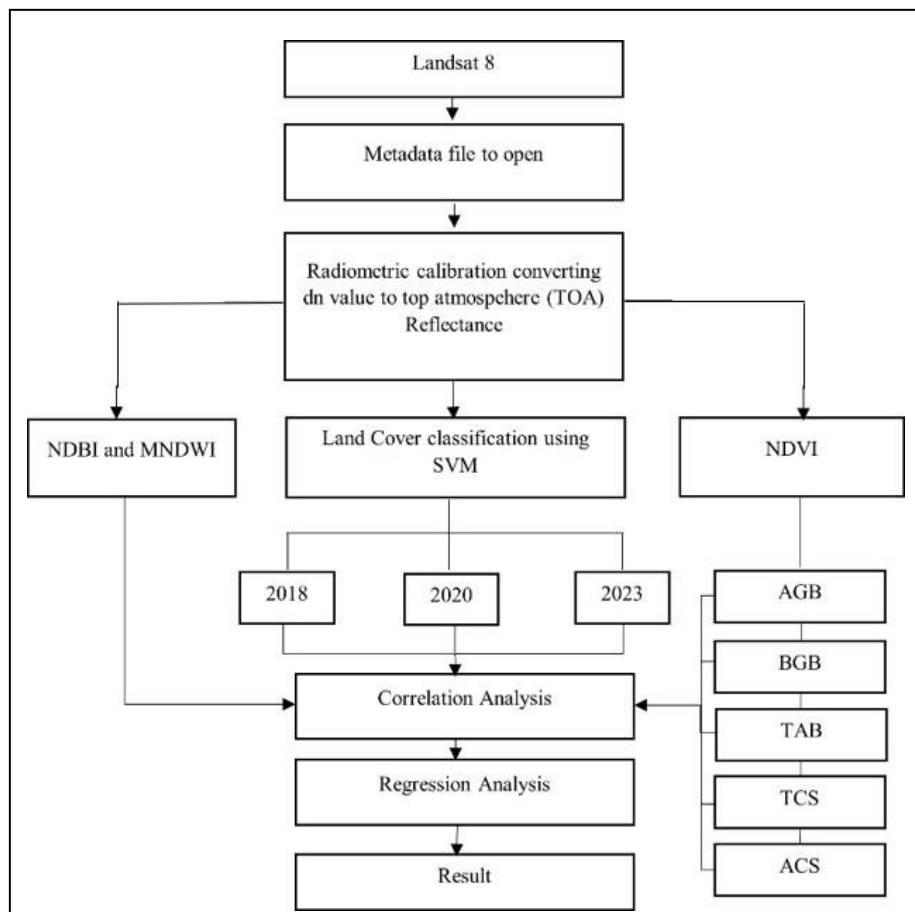


Figure 3: Research flowchart

3 RESULTS AND DISCUSSION

3.1 MULTI-TEMPORAL LAND COVER CLASSIFICATION

Landsat 8 OLI images, acquired on various dates in 2018, 2020, and 2023 (Figure 4), were processed and classified into three distinct land cover types: Mangrove, Urban, and Waterbody. This classification was achieved using spectral data from the imagery to differentiate between the land cover categories. The resulting classified maps, which show the distribution and extent of each land cover type, are presented in Figure 5. From the results of accuracy assessment, overall accuracies for the Landsat 8 OLI imagery were assessed for the years 2018, 2020, and 2023. The accuracy for 2018 was 96.9%, indicating a high level of precision in categorizing the land cover types. In 2020, the accuracy was 96.4%, which still reflects strong classification performance, though slightly lower than 2018. For 2023, the accuracy increased to 97.7%, demonstrating the effectiveness and consistency of the classification process over time. These accuracy metrics highlight the robustness and reliability of the land cover classification in distinguishing between Mangrove, Urban, and Waterbody types across the different years. Meanwhile the kappa statistics values for each year are 0.87, 0.83, and 0.84. The classification for this area mostly indicates good classification performance, with Kappa values more than 0.80 (based on the findings from Lillesand et al., 2004; Jensen 2005). This shown on the Table 3-5 below. The land cover in the area primarily consists of mangrove forest. There has been a change in land cover from mangrove forest to urban development in the selected area.

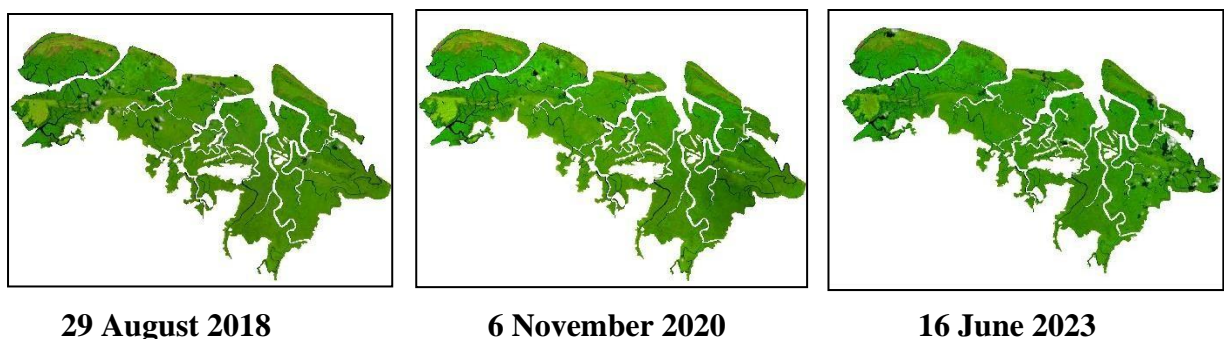
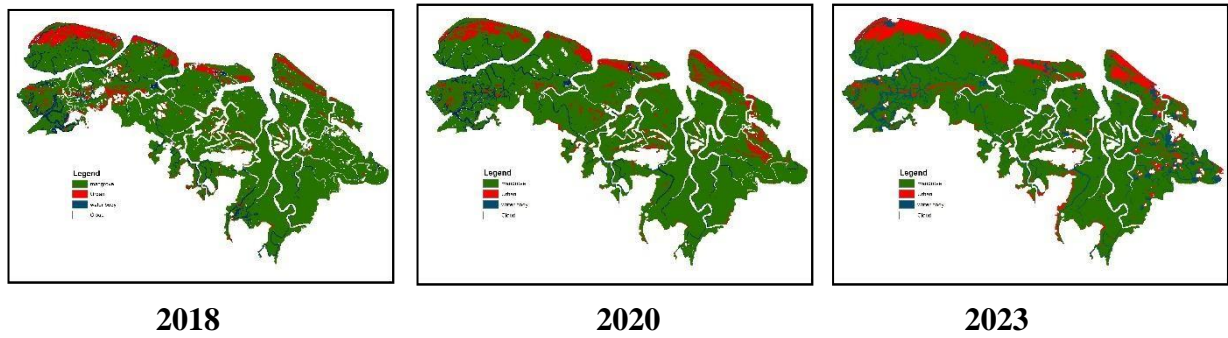


Figure 4: Multiple date Landsat 8 OLI imageries


Figure 5: Land Cover Map
Table 3: Landcover classes 2018 - 2023

Land Cover / Year	Area (ha)		
	2018	2020	2023
Mangrove	208.0	217.0	219.0
Urban	200.0	230.0	260.0
Water body	13.0	13.0	13.0
Cloud	14.0	13.0	13.0

Table 4: Confusion Matrix (2018)

Year: 2018, Overall Accuracy: 96.9 %, Kappa Statistics: 0.865					
Land Cover	Mangrove	Urban	Water body	Total	User Accuracy
Mangrove	140.000	3.000	0.000	143.000	0.979
Urban	2.000	8.000	0.000	10.000	0.800
Water body	0.000	0.000	10.000	10.000	1.000
Total	142.000	11.000	10.000	163.000	0.000
Producer Accuracy	0.986	0.727	1.000	0.000	0.969

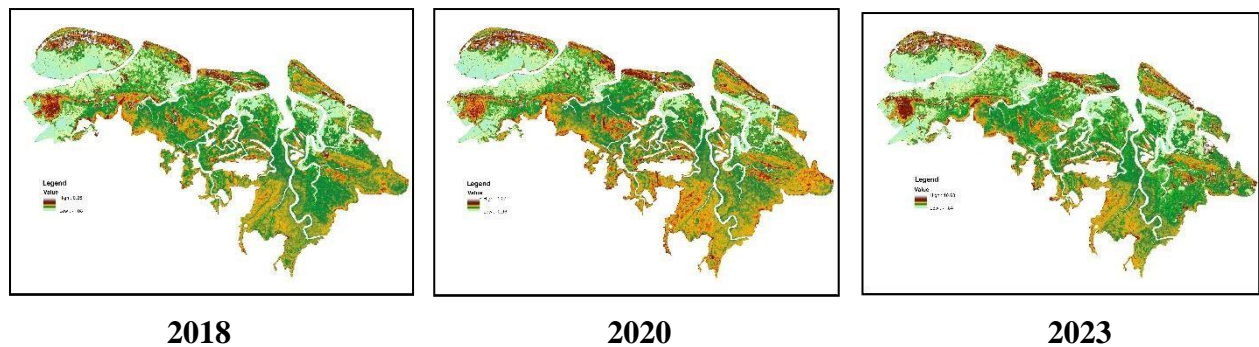
Table 5: Confusion Matrix (2020)

Year: 2020, Overall Accuracy: 96.4 %, Kappa Statistics: 0.831					
Land Cover	Mangrove	Urban	Water body	Total	User Accuracy
Mangrove	143.000	2.000	0.000	145.000	0.986
Urban	3.000	6.000	1.000	10.000	0.600
Water body	0.000	0.000	10.000	10.000	1.000
Total	146.000	8.000	11.000	165.000	0.000
Producer Accuracy	0.979	0.750	0.909	0.000	0.964

Table 6: Confusion Matrix (2023)

Year: 2023, Overall Accuracy : 97.7%, Kappa Statistics : 0.835					
Land Cover	Mangrove	Urban	Water body	Total	User Accuracy
Mangrove	280.000	6.000	0.000	286.000	0.979
Urban	1.000	9.000	0.000	10.000	0.900
Water body	0.000	0.000	10.000	10.000	1.000
Total	281.000	15.000	10.000	306.000	0.000
Producer Accuracy	0.996	0.600	1.000	0.000	0.977

The Normalized Difference Built-up Index (NDBI) was derived from Landsat 8 OLI imagery by utilizing the specific spectral bands corresponding to the Near Infrared (NIR) and Short-Wave Infrared (SWIR) wavelength regions. Specifically, the NIR band (Band 5) and the SWIR band (Band 6) were used to calculate the NDBI, which is an index designed to highlight built-up areas by measuring the difference between the reflectance of these two bands. This index is particularly useful for identifying urbanized regions, as built-up areas tend to reflect more in the SWIR band compared to the NIR band. The resulting NDBI values help in distinguishing urban areas from other land cover types, contributing to urban planning and land use studies. NDBI values will be ranged from -1 to 1, where NDBI value closer to 1 indicates a high building density condition, while a negative NDBI value means that the area is classified as a non-built-up area (Naserikia et al., 2019). This relationship is used for finding the area of built-up area class.


Figure 6: Normalized Difference Built-up Index (NDBI) Classification maps

The Modified Normalized Difference Water Index (MNDWI) was applied to Landsat 8 OLI imagery to accurately identify water bodies, including areas where vegetation, such as crops, is submerged under water. The MNDWI leverages specific spectral bands from the Landsat 8 OLI sensor, particularly the green band (Band 3) and the Short-Wave Infrared (SWIR) band (Band 6),

to enhance the detection of water features. By highlighting water bodies and suppressing the reflectance of built-up and vegetation areas, the MNDWI provides a clear distinction of water-covered regions, making it particularly useful for identifying and monitoring flooded agricultural fields and other water-related land cover. The visual representation of the identified water body areas, as determined by the MNDWI, is shown in Figure 7, illustrating the effectiveness of this index in mapping submerged vegetation and water bodies.

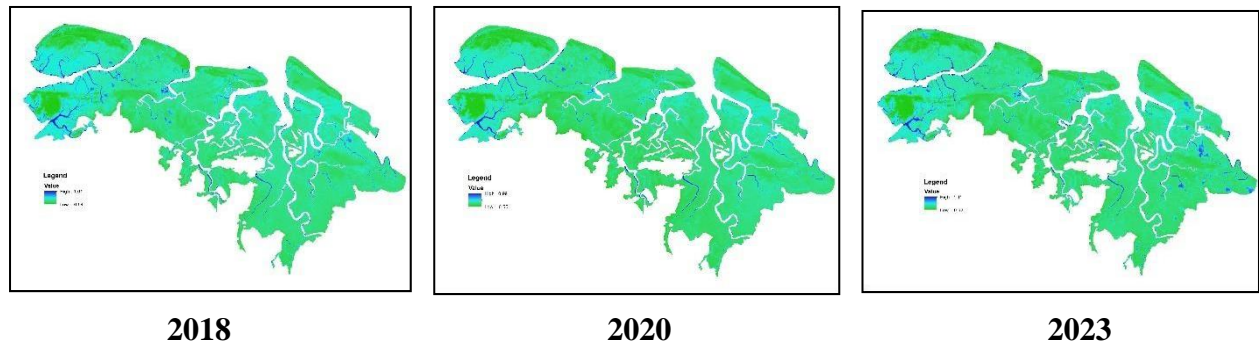


Figure 7: Modified normalized difference water index (MNDWI) Classification maps

The Normalized Difference Vegetation Index (NDVI) technique is used to determine vegetation index and changes in plant coverage, such as shifts in tree canopies, leaf area index, and overall biomass using specific band combinations of remote sensing data. In the field of remote sensing, it's essential to understand that the Earth's surface reflects different bands. When vegetation is actively carrying out photosynthesis, it absorbs most of the red band (Near Infrared Reflectance). By analyzing the reflectance of the red and infrared bands in a multispectral image, can effectively observe and measure the density of green growth in vegetation. Understanding these principles is crucial for accurate remote sensing analysis (M. A. Ganie,2016). This method allows interpretation of land resources through the computation of NDVI for land cover classification is shown in Figure 8. In this analysis, we discovered that the mangrove forest covers an area of approximately 219 hectares within the research area. Mangrove forest has been identified using NDVI for the years 2018,2020 and 2023. This index was selected by considering the capacity gained from estimating carbon stocks in mangrove forests. Among the various vegetation indices, NDVI is widely used for investigating carbon dynamics. Less dense vegetation such as shrubs or less mature mangroves has moderate NDVI values, approximately 0.2 to 0.5, while high NDVI values approximately 0.6 to 0.9, correspond to dense vegetation found in mangrove forests during the peak growth phase. Therefore, a higher NDVI indicates a greater amount of green vegetation on the ground. The NDVI of the non-vegetation class is generally lower than that of the vegetation class (M. A. Ganie,2016).

The NDVI value from 2018 to 2023 indicates that the improved vegetation health and increased in vegetation density with higher biomass per unit area.

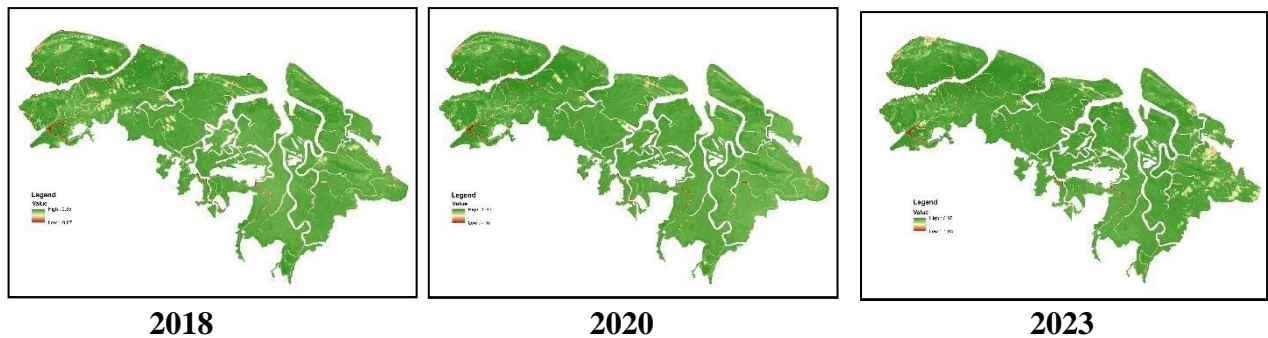


Figure 8: Normalized Difference Vegetation Index (NDVI) Classification maps

Tree biomass is divided into Above Ground Biomass (AGB) and Below Ground Biomass (BGB). AGB includes the trunk, branches, leaves, and reproductive structures, playing a key role in photosynthesis and carbon storage. BGB consists of the root system, which is crucial for structural support and nutrient absorption. While AGB is often more visible, BGB typically makes up 20-30% of total biomass and is vital for the tree's health and stability. The balance between AGB and BGB is essential for a tree's ability to adapt to environmental changes, with implications for ecological research and forest management.

Tables 7 through Table 9 present the Above Ground Biomass (AGB) values, demonstrating a progressive increase over the years. In 2018, the AGB was recorded at 56.45 ± 20.87 tons per hectare. By 2020, this value increased to 64.58 ± 23.09 tons per hectare, reflecting an upward trend in biomass accumulation. In 2023, the AGB further increased to 71.80 ± 25.67 tons per hectare. These figures indicate a consistent rise in AGB over time, with the associated standard deviations highlighting the variability in biomass distribution across the measured areas. Determining the value of Above Ground Biomass (AGB) is a crucial step in planning for the protection and optimal management of natural mangrove resources, as emphasized by Medeiros and Sampaio (2008). Accurate measurement of AGB helps in assessing the health and productivity of mangrove ecosystems, guiding conservation efforts, and ensuring sustainable use of these vital coastal resources.

Differences in Above Ground Biomass (AGB) and Below Ground Biomass (BGB) values are observed among mangrove species due to several influencing factors. These include geographical location, which affects environmental conditions such as salinity and soil type; tree density, which impacts competition for resources; and ecological factors, such as species-specific growth patterns and adaptations. These variations highlight the importance of considering these factors in the management and conservation of mangrove ecosystems.

Total accumulated biomass (TAB) refers to the total amount of biomass both above and below the soil surface (Amandangi,2017). In Trusan Kinabatangan, Sabah, the Total Above Biomass(TAB) was recorded at 57.00 ± 20.82 tons per hectare in 2018. By 2020, this value had increased to 65.10 ± 23.02 tons per hectare. By 2023, the TAB further rose to 72.31 ± 25.58 tons per hectare. This upward trend in TAB indicates a significant increase in carbon stock over the years, reflecting changes in biomass accumulation within the mangrove ecosystem of the region. When the BGB to AGB ratio is higher, it indicates substantial root growth compared to trunk growth (Amandangi,2017). Plant biomass is directly linked to photosynthesis, as biomass increases when plants absorb CO_2 and convert it into organic compounds through photosynthesis. The biomass in each part of the plant increases in proportion to the tree's diameter. The capacity of trees to sequester carbon from the air influenced by both tree diameter and tree height (Fu W,2011).

The quantity of carbon can be estimated by converting biomass to carbon, using the IPCC default carbon fraction of 0.47. Belowground tree root biomass is commonly estimated as a ratio of the aboveground tree biomass (Sarah,2016). In 2018, the total carbon stock (TCS) estimated from remote sensing measurements in the study area was 26.79 ± 9.79 tons per hectare. By 2020, this figure had risen to 30.60 ± 10.82 tons per hectare, indicating an increase in carbon storage over a two-year period. This upward trend continued, with the TCS reaching 33.99 ± 12.02 tons per hectare by 2023.

This progressive increase in TCS reflects a cumulative rise in carbon sequestration, suggesting enhanced biomass accumulation and improved carbon retention within the ecosystem over the studied years. The increasing carbon stock values underscore the effectiveness of the area in capturing and storing atmospheric carbon, which is crucial for climate change mitigation efforts. The variability in the TCS values, as indicated by the standard deviations, highlights the spatial heterogeneity and potential measurement uncertainties in the remote sensing data. There is a difference in carbon stock value between natural mangrove forests and replantation mangroves in ex-ponds. It was found that carbon stock produced by natural mangroves is higher than replantation

mangroves in ex-ponds (Sidik et al. 2014). From this study, the data revealed a progressive annual increase in carbon stock estimates: from 26.79 ± 9.79 tons per hectare in 2018, to 30.60 ± 10.82 tons per hectare in 2020, and further to 33.99 ± 12.02 tons per hectare by 2023. This consistent upward trend demonstrates the effectiveness of the remote sensing methodology in accurately capturing the accumulation of carbon in mangrove ecosystems. The increasing carbon stock values reflect enhanced carbon sequestration and storage capacity of the mangroves, validating the remote sensing approach as a reliable tool for monitoring and assessing long-term changes in carbon stocks.

The study findings indicate that the variation in carbon stock in Trusan Kinabatangan, Sabah, is primarily influenced by the growth dynamics and age of the mangrove trees. As the trees mature, their biomass accumulates, which leads to an increase in carbon sequestration capacity. This growth trajectory results in a progressive rise in carbon stock values over the years. The correlation between tree age, biomass accumulation, and carbon stock emphasizes the critical role of mangrove tree growth in determining overall carbon storage. Understanding these dynamics is essential for accurately assessing carbon sequestration potential and implementing effective management strategies for mangrove conservation and climate change mitigation. Approximately 70% of the variability in carbon stock is attributed to the age of the trees (Estrada and Soares, 2017), as well as the species, management forest, and climate (Kairo et al., 2008).

Scientific studies reveal that the Amount of CO₂ Sequestration (ACS) in Trusan Kinabatangan, Sabah, increased from 98.32 ± 35.92 tons per hectare in 2018 to 124.73 ± 44.12 tons per hectare in 2023. This result indicates a significant enhancement in the carbon sequestration capacity of the mangrove ecosystem. The rise in ACS values over time is attributed to the ongoing growth and biomass accumulation of mangrove trees, which effectively sequester more CO₂. The variation in ACS estimates, reflected in the standard deviations, accounts for spatial heterogeneity and potential measurement errors inherent in remote sensing data. These results underscore the utility of remote sensing technologies in accurately assessing temporal changes in carbon sequestration and emphasize the critical role of mangrove forests in global carbon cycling and climate change mitigation.

Table 7: Average Value of NDVI, AGB, BGB, TAB, TCS and ACS 2018

Year 2018			
Average Value	Statistics (t Ha ⁻¹)		
	Mean±SD	Max	Min
NDVI	0.68±0.12	0.86	-0.88
AGB	56.45±20.87	144.02	0
BGB	0.55±2.28	546.25	0.42
TAB	57.00±20.82	546.25	1.52
TCS	26.79±9.79	256.02	0.72
ACS	98.32±35.92	942.23	2.63

Table 8: Average Value of NDVI, AGB, BGB, TAB, TCS and ACS 2020

Year 2020			
Average Value	Statistics (t Ha ⁻¹)		
	Mean±SD	Max	Min
NDVI	0.71±0.12	0.85	-1.01
AGB	64.58±23.09	136.73	0
BGB	0.52±1.72	561.55	0.42
TAB	65.10±23.02	561.55	1.52
TCS	30.60±10.82	263.93	0.72
ACS	112.30±39.70	968.62	2.63

Table 9: Average Value of NDVI, AGB, BGB, TAB, TCS and ACS 2023

Year 2023			
Average Value	Statistics (t Ha ⁻¹)		
	Mean±SD	Max	Min
NDVI	0.72±0.13	0.87	-1.03
AGB	71.80±25.67	156.62	0
BGB	0.52±1.56	539.54	0.41
TAB	72.31±25.58	539.54	1.52
TCS	33.99±12.02	253.58	0.72
ACS	124.73±44.12	930.65	2.63

Figure 9 provides a detailed overview of the distribution and annual variations of Total Above Biomass (TAB), Total Carbon Stock (TCS), and Amount of CO₂ Sequestration (ACS) in Trusan Kinabatangan, Sabah for the years 2018, 2020, and 2023. The data demonstrate that the values of TAB, TCS, and ACS fluctuate annually, influenced by the different types of mangroves, including those that are naturally occurring and those that have been restored. Specifically, in natural mangrove forests, the average values of TAB, TCS, and ACS exhibit a consistent increase each

year. This trend is primarily due to the progressive growth and maturation of the mangrove trees, leading to greater biomass accumulation and enhanced carbon sequestration over time.

The Normalized Difference Vegetation Index (NDVI) values calculated for each pixel in satellite imagery can be used to estimate carbon stock in the area. NDVI, which measures vegetation density and health by comparing the reflectance in the red and near-infrared bands, provides an indication of vegetation cover and biomass. Variability in NDVI values can lead to diverse outcomes in carbon stock estimates due to differences in vegetation type, growth stages, and environmental conditions such as soil moisture and nutrient availability. Accurate estimation of carbon stock using NDVI requires considering these factors, as they influence the relationship between NDVI values and actual carbon sequestration. The relationship between NDVI and Above Ground Biomass (AGB) exhibits complexities that can influence biomass estimation. While linear regression typically shows higher correlation coefficients between NDVI and AGB, it may not fully capture the true distribution of biomass, particularly at NDVI values near zero. At low NDVI values, the linear model may inadequately represent the non-linear or saturated relationships between vegetation density and biomass, potentially leading to less accurate biomass estimates.

To ensure accurate estimation of carbon stock in mangrove environments using remote sensing methods, conducting field testing is essential. Field measurements provide ground-truth data that validate and calibrate remote sensing results, addressing potential discrepancies caused by variations in vegetation types, soil conditions, and sensor limitations. This ground-truthing process helps improve the reliability and precision of carbon stock estimates derived from remote sensing technologies. While the NDVI method may not be the optimal choice, it demonstrates relatively consistent accuracy with various levels of radiometric correction (Wicaksono et al., 2011). Additionally, it is crucial to utilize high-resolution image data to effectively assess the condition and dynamics of mangroves (Rodriguez and Feller, 2004), classify tree species based on their reflectance value (Wang et al., 2004; Dahdouh-Guebas et al., 2005), and cater to other essential requirements.

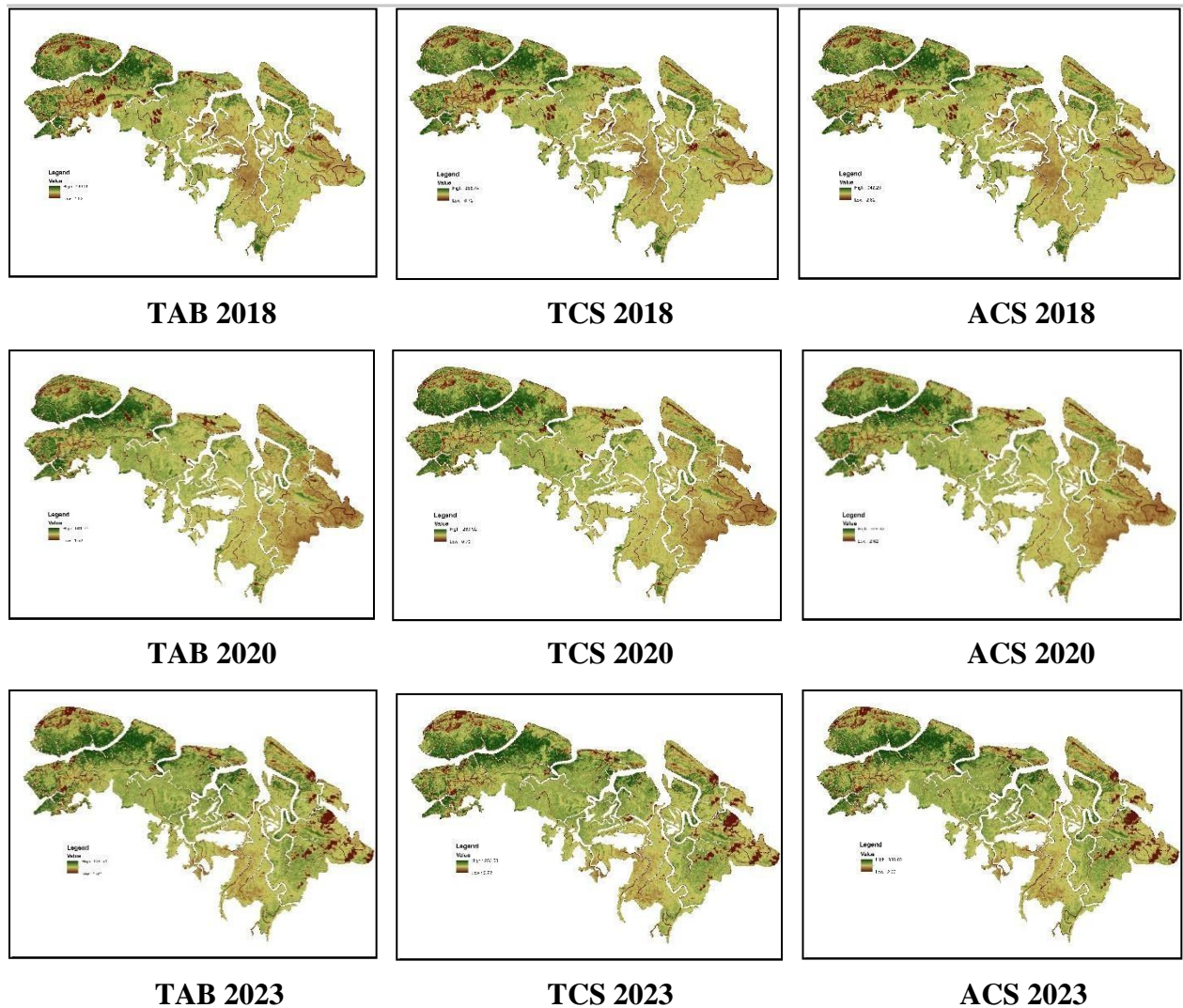


Figure 9: Map of value and distribution of TAB, TCS and ACS in Trusan Kinabatangan, Sabah in 2018 to 2023

Figure 10 shown graph pattern distribution of value NDVI, TCS and ACS from years 2018, 2020 and 2023. The NDVI values have progressively increased from 0.68 in 2018 to 0.72 in 2023. This trend suggests that vegetation health and greenness have improved over the years. Higher NDVI values generally indicate more vigorous, healthier vegetation with denser foliage. The TCS values have risen from 26.79 in 2018 to 33.99 in 2023, showing a steady increase in the amount of carbon stored in the ecosystem. This trend suggests that the area has become more effective at sequestering carbon, likely due to an increase in mangrove density or natural regrowth of mangrove which enhances carbon storage of the area. The ACS values have consistently risen from 98.32 in 2018 to 124.73 in 2023, reflecting a steady increase in the carbon stored over the years. Comparatively, from 2018 to 2023, biomass accumulation significantly increases by 26.41 tons of carbon per hectare or 27% in a similar area. This suggests an expansion of aboveground biomass, likely due to an increase in tree cover, plant density, or vegetation health. Overall, this is a positive sign for ecosystem health, climate mitigation, and sustainable land management practices.

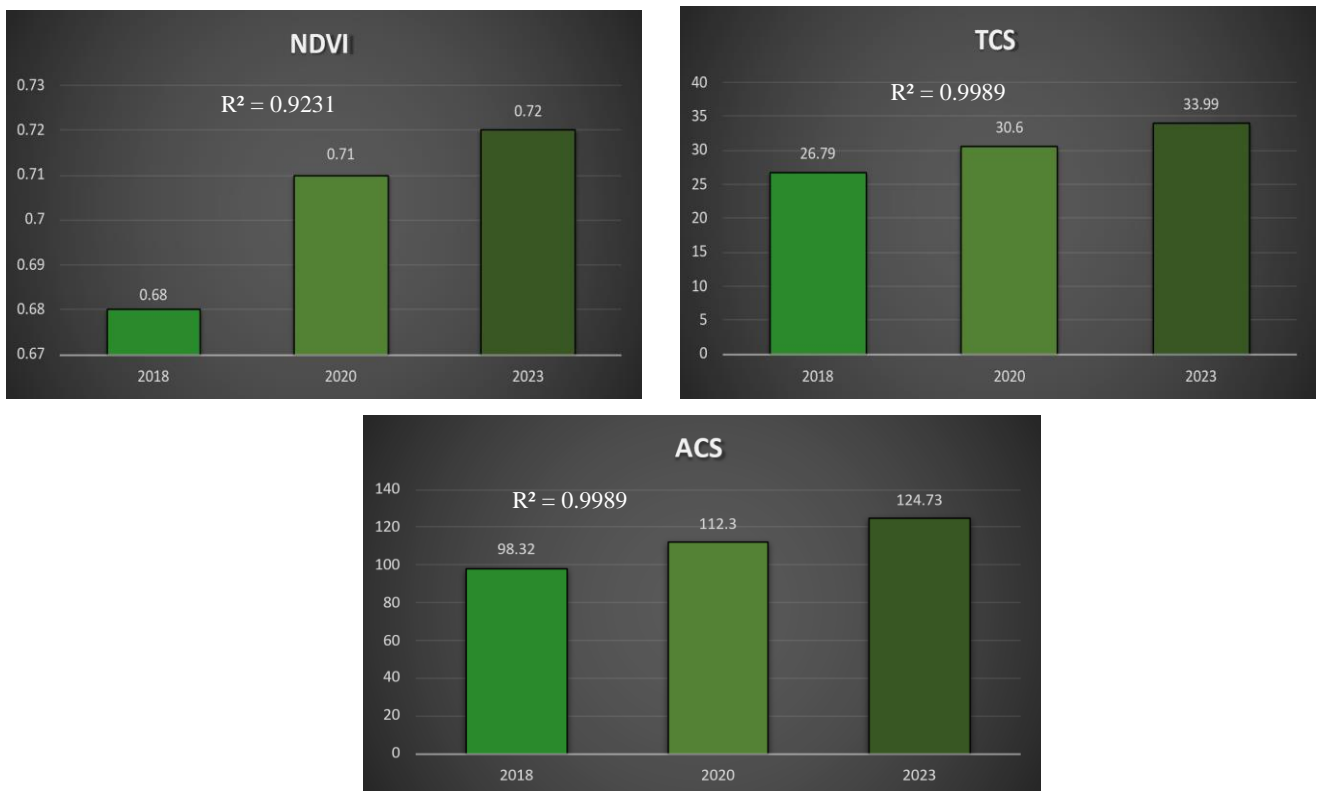


Figure 10: Graph showing pattern distribution value of NDVI, TCS and ACS from the years 2018, 2020 and 2023 in the study area.

CONCLUSION

Recent extreme climate changes, such as increased global temperatures and more frequent severe weather events, have intensified environmental challenges, necessitating effective interventions. Despite the implementation of various international policies and actions such as the Paris Agreement's targets for reducing greenhouse gas emissions and promoting carbon sinks, there is ongoing debate about their effectiveness in enhancing carbon sequestration. For instance, while forest conservation and reforestation efforts aim to increase carbon storage, studies have shown that actual carbon sequestration rates can be influenced by factors such as forest management practices, land-use changes, and climate variability. This ongoing debate highlights the need for rigorous assessment and refinement of these strategies to ensure they achieve their intended goals of improving carbon capture and mitigating climate change. The study results show that increases in Above Ground Biomass (AGB), Below Ground Biomass (BGB), and Total Above Biomass (TAB) indicate a significant growth in biomass within the area. This growth reflects a healthier and more vigorous vegetation structure. The enhanced biomass levels are associated with an improved carbon sequestration capacity of the ecosystem, suggesting that the mangrove forest is increasingly effective in capturing and storing atmospheric carbon. This improvement underscores the ecosystem's role in mitigating climate change through enhanced carbon storage. To enhance the

accuracy of carbon sequestration assessments in mangrove ecosystems using remote sensing, several strategies should be employed. First, improving the quality of remote sensing data is essential for capturing precise and detailed vegetation and carbon stock information. Second, refining biomass and carbon models by developing allometric equations tailored to specific mangrove species and regional characteristics will enhance estimation accuracy. Third, validating remote sensing-based biomass models with ground-truth data is crucial for ensuring their reliability. Fourth, integrating climate and soil data can provide a more comprehensive understanding of factors influencing carbon sequestration. Additionally, establishing long-term monitoring programs will enable ongoing observation of biomass and carbon stock changes, offering a thorough assessment of sequestration potential. Finally, collaborating with experts from various research institutions will enrich the evaluation process and improve overall assessment quality.

ACKNOWLEDGMENT

We extend our sincere gratitude to the United States Geological Survey (USGS) for supplying the Landsat 8 data used in this study. The Landsat 8 Operational Land Imager (OLI) and Thermal Infrared Sensor (TIRS) provided crucial high-resolution imagery, enabling precise analysis and valuable insights into our research. We appreciate the USGS's commitment to advancing remote sensing technology and making these data available to the scientific community. We also wish to thank the Malaysian Space Agency (MYSA) for their support and the opportunity to conduct this study. Their contributions have been instrumental in advancing our research.

REFERENCE

- Alongi, D. M. (2014). Carbon cycling and storage in mangrove forests. *Annual Review of Marine Science*, 6, 195-219. <https://doi.org/10.1146/annurev-marine-010213-135020>
- Amandagi, R. (2017). **Remote sensing for mangrove forest mapping and monitoring: A case study of Indonesia**. *Journal of Environmental Science and Technology*, 10(3), 115-122.
- Atwood, T. B., Connolly, R. M., Ritchie, E. G., Lovelock, C. E., Heithaus, M. R., Hays, G. C., & Duarte, C. M. (2017). **Global patterns in mangrove soil carbon stocks and losses**. *Nature Climate Change*, 7(7), 523-528. <https://doi.org/10.1038/nclimate3326>
- Dahdouh-Guebas, F., Koedam, N., & Cannicci, S. (2005). **Mangrove rehabilitation in Kenya: An evaluation of forest structure and carbon sequestration capacity**. *Global Ecology and Biogeography*, 14(5), 453-464. <https://doi.org/10.1111/j.1466-822X.2005.00167.x>
- Donato, D. C., Kauffman, J. B., Murdiyarso, D., Kurnianto, S., Stidham, M., & Kanninen, M. (2011). **Mangroves among the most carbon-rich forests in the tropics**. *Nature Geoscience*, 4(5), 293-297. <https://doi.org/10.1038/ngeo1123>
- Estrada, G. C. D., & Soares, M. L. G. (2017). **Carbon sequestration in mangrove ecosystems: A case study from southeastern Brazil**. *Journal of Coastal Research*, 33(2), 335-342. <https://doi.org/10.2112/JCOASTRES-D-16-00057.1>
- Fatoyinbo, T. E., Simard, M., Washington-Allen, R. A., & Shugart, H. H. (2008). **Landscape-scale extent, height, biomass, and carbon estimation of Mozambique's mangrove forests with Landsat ETM+ and Shuttle Radar Topography Mission elevation data**. *Remote Sensing of Environment*, 112(5), 1535-1548. <https://doi.org/10.1016/j.rse.2007.08.015>
- Fu, W., Jiang, P., & Zhou, G. (2011). **The role of non-forest land use in carbon sequestration in China's forests: Based on remote sensing and ecological models**. *Forest Ecology and Management*, 262(3), 370-377. <https://doi.org/10.1016/j.foreco.2011.03.036>

Ganie, M. A., & Bhatt, B. P. (2016). **Above-ground biomass and carbon stocks of tree species in tropical forests of Eastern Himalaya, India.** *Journal of Forestry Research*, 27(2), 223-230. <https://doi.org/10.1007/s11676-015-0164-6>

Giri, C. (2016). **Remote sensing of mangroves in the aftermath of the 2004 Indian Ocean tsunami: Lessons learned and future outlook.** *ISPRS Journal of Photogrammetry and Remote Sensing*, 115, 83-89. <https://doi.org/10.1016/j.isprsjprs.2015.10.004>

Kairo, J. G., Bosire, J., Lang'at, J., & Kirui, B. (2008). **Allometry and biomass distribution in replanted mangrove plantations at Gazi Bay, Kenya.** *Aquatic Botany*, 89(3), 251-259. <https://doi.org/10.1016/j.aquabot.2008.02.010>

Lu, D. (2006). **The potential and challenge of remote sensing-based biomass estimation.** *International Journal of Remote Sensing*, 27(7), 1297-1328. <https://doi.org/10.1080/01431160500486732>

Medeiros, J. S., & Sampaio, E. V. S. B. (2008). **Allometry of aboveground biomass in mangrove species in Brazil.** *Wetlands Ecology and Management*, 16(4), 323-330. <https://doi.org/10.1007/s11273-007-9063-z>

Naserikia, M., Hashim, M., Zolfaghari, H., & Mahmud, A. R. (2019). **Monitoring mangrove forest changes using remote sensing and GIS: A case study of Kuala Langat, Malaysia.** *Global Ecology and Conservation*, 20, e00702. <https://doi.org/10.1016/j.gecco.2019.e00702>

Rodriguez, M. A., & Feller, I. C. (2004). **Variation in mangrove biomass and carbon storage with salinity and tidal inundation in a tropical estuary.** *Estuarine, Coastal and Shelf Science*, 60(1), 99-110. <https://doi.org/10.1016/j.ecss.2004.02.007>

Sarah, M. (2016). **The role of mangrove forests in carbon sequestration and climate change mitigation.** *Journal of Coastal Conservation*, 20(4), 345-352.

Sidik, F., Lovelock, C. E., & Alongi, D. M. (2014). **Carbon sequestration and fluxes of tidal swamps dominated by the mangrove *Avicennia marina* in the Indo-Pacific region.** *Wetlands Ecology and Management*, 22(2), 177-187. <https://doi.org/10.1007/s11273-013-9313-7>

TM/Landsat 5 Images for The Araguaia River - Brazil. *Remote Sensing Letters*, 47-56.

Wang, Y., Li, X., & Zhang, Y. (2004). **Mangrove forest biomass and carbon storage in southern China.** *Wetlands Ecology and Management*, 12(4), 281-289.
<https://doi.org/10.1023/B:WETL.0000049808.15497.8a>

Wicaksono, B., Syamsuddin, F., & Hadi, S. (2011). **Assessment of mangrove forest biomass and carbon stock using remote sensing and ground-based measurements in Indonesia.** *International Journal of Remote Sensing*, 32(23), 7737-7754.
<https://doi.org/10.1080/01431161.2010.496649>